



Short Communication

Microfocus x-ray fluorescence mapping of tumour penetration by an organo-osmium anticancer complex

Carlos Sanchez-Cano^{a,*}, Isolda Romero-Canelón^{a,b}, Kalotina Geraki^c, Peter J. Sadler^{a,*}^a Department of Chemistry, University of Warwick, Coventry CV4 7AL, UK^b School of Pharmacy, University of Birmingham, Birmingham B15 2TT, UK^c Diamond Light Source, Harwell Science and Innovation Campus, Didcot, Oxon OX11 0DE, UK

ARTICLE INFO

Keywords:

Organometallic metalodrugs
3D spheroids
Tumour penetration
Elemental mapping
X-ray fluorescence

ABSTRACT

Microfocus synchrotron x-ray fluorescence (SXRF) imaging focussed on detection of the Os L_{III} edge shows that the organo-osmium metalodrugs candidate $[(\eta^6\text{-}p\text{-cym})\text{Os}(\text{Azpy-NMe}_2)\text{I}]^+$ ($p\text{-cym} = p\text{-cymene}$, $\text{Azpy-NMe}_2 = 2\text{-}(p\text{-}([\text{dimethylamino}]\text{phenylazo})\text{pyridine})$) **1** penetrates efficiently into the interior of A2780 human ovarian cancer cell spheroids, a model for a solid tumour. The accompanying changes in Zn and Ca distribution suggest that the complex causes nuclear damage and initiates signalling events for cell death, consistent with findings for cultured cancer cell monolayers. Such tumour penetration is likely to be important for combatting resistance to chemotherapy, which is becoming a problem for current clinical platinum drugs.

There is a clinical need for new anticancer treatments capable of overcoming platinum resistance [1]. New generations of drug candidates with novel mechanisms of action need to penetrate into the interior of tumours since this is likely to be a major factor in determining resistance to chemotherapy [2]. Hence, metalodrugs candidates should be capable of reaching the core of treated tumours.

Organometallic Ru, Ir and Os-‘piano-stool’ complexes are a class of compounds with promising anticancer properties [3–13]. In particular, $[(\eta^6\text{-}p\text{-cym})\text{Os}(\text{Azpy-NMe}_2)\text{I}]^+$ ($p\text{-cym} = p\text{-cymene}$, $\text{Azpy-NMe}_2 = 2\text{-}(p\text{-}([\text{dimethylamino}]\text{phenylazo})\text{pyridine})$) **1** (Chart 1) exhibits potent activity towards a wide range of cancer cell lines. It has a different mechanism of action to cisplatin and is capable of overcoming resistance to clinical platinum drugs *in vitro*. It also shows promising antitumour activity *in vivo* [14,15].

We have demonstrated that **1** is a relatively inert prodrug that can be activated by hydrolysis of the Os–I bond under intracellular reductive conditions, generating the more reactive Os–OH adduct **[1-OH]**. Interestingly, the chlorido analogue **[1-Cl]**, behaves similarly to **1**, but hydrolyses more rapidly, and is $10\times$ less active in inhibiting the proliferation of cancer cells [16]. Complex **1** rapidly generates large quantities of reactive oxygen species (ROS) inside cells through mitochondrial pathways [17,18]. Using synchrotron X-ray fluorescence (SXRF), we showed that osmium from **1** is concentrated in small

organelles within the cytosol of treated cells, possibly mitochondria, leading to extensive nuclear damage, and mobilisation of Ca from the endoplasmic reticulum (a signalling event for cell death) [19].

The interaction of **1** with solid tumours has yet to be investigated. Here we use 3D spheroids as tumour models that can be readily cultured *in vitro* [20,21]. They provide useful systems for the study of tumour growth inhibition and drug penetration. Tumour penetration by metalodrugs has been studied by SXRF [22–24] and other techniques such as Laser Ablation Inductively Coupled Plasma Mass Spectrometry (LA-ICP-MS) [25] or Matrix-Assisted Laser Desorption/Ionization Mass Spectrometric Imaging (MALDI-MSI) [26] which allow direct mapping of metals in biological samples, including 3D spheroid solid tumour models.

We have acquired SXRF elemental maps of A2780 human ovarian carcinoma spheroids to study the ability of organo-osmium drug candidate **1** to penetrate into solid tumours and its effect on the distribution of natural metal ions.

A2780 ovarian carcinoma 3D spheroids were generated by growing cells for 5 days in U-bottom cell-repellent 96 well plates. The size of the tumour models was controlled by altering the initial cell density. 1000–5000 cells/well yielded spheroids with a diameter $406 \pm 6\ \mu\text{m}$ – $560 \pm 8\ \mu\text{m}$ (Fig. S1). For tumour growth inhibition assays, 2500 cells were seeded and grown for 3 days, yielding spheroids of

Abbreviations: SXRF, Synchrotron x-ray fluorescence; $p\text{-cym}$, $p\text{-cymene}$; Azpy-NMe_2 , 2- $(p\text{-}([\text{dimethylamino}]\text{phenylazo})\text{pyridine})$; ROS, Reactive Oxygen Species; LA-ICP-MS, Laser Ablation Inductively Coupled Plasma Mass Spectrometry; MALDI-MSI, Matrix-Assisted Laser Desorption/Ionization Mass Spectrometric Imaging; $\text{IC}_{50\text{-sph}}$, 50% inhibition concentrations for 3D spheroids; IC_{50} , 50% inhibition concentrations; ROIs, Regions of interest; ER, Endoplasmic Reticulum; XAS, X-ray Absorption Spectroscopy; XANES, X-ray Absorption Near Edge Structure; EXAFS, Extended X-Ray Absorption Fine Structure

* Corresponding authors.

E-mail addresses: c.sanchez@warwick.ac.uk (C. Sanchez-Cano), p.j.sadler@warwick.ac.uk (P.J. Sadler).<https://doi.org/10.1016/j.jinorgbio.2018.04.014>

Received 23 March 2018; Received in revised form 21 April 2018; Accepted 21 April 2018

Available online 25 April 2018

0162-0134/© 2018 The Authors. Published by Elsevier Inc. This is an open access article under the CC BY license (<http://creativecommons.org/licenses/by/4.0/>).

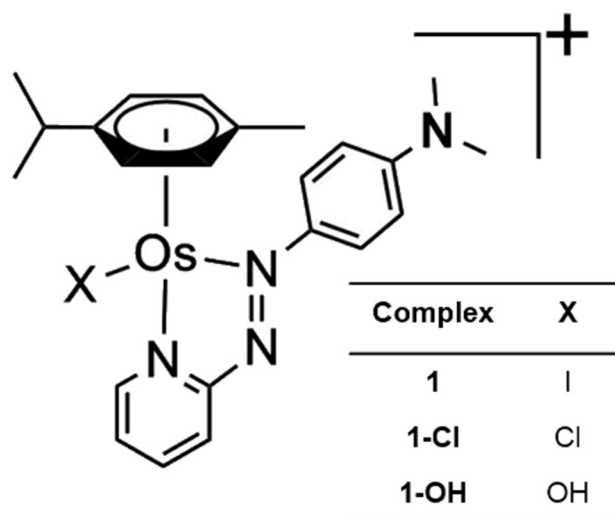


Chart 1. Structures of $[(\eta^6\text{-p-cym})\text{Os}(\text{Azppy-NMe}_2)\text{I}]^+$ [1] and related complexes.

Table 1

Growth inhibition ($\text{IC}_{50\text{-sph}}$ μM) of A2780 human ovarian carcinoma 3D spheroid tumour models.

Complex	$\text{IC}_{50\text{-sph}}$ (μM) exposure time		
	16 h	24 h	48 h
Cisplatin	191 ± 9	108 ± 8	79.8 ± 0.2
1-Cl	86 ± 4	47 ± 2	22.3 ± 0.3
1	9.7 ± 0.3	3.5 ± 0.6	1.43 ± 0.04

Table 2

Antiproliferative activity (IC_{50} μM) towards monolayers of A2780 human ovarian carcinoma cancer cells.

Complex	IC_{50} (μM) exposure time		
	16 h	24 h	48 h
Cisplatin	90 ± 11	23.7 ± 0.7	15 ± 0.9
1-Cl	14 ± 1	5.5 ± 0.4	2.0 ± 0.02
1	0.8 ± 0.2	0.5 ± 0.1	0.10 ± 0.01

$275 \pm 6 \mu\text{m}$ diameter. They were exposed to **1** for 16–48 h, and ATP content was measured using a luminescence assay to determine cell viability in the 3D spheroids. Cisplatin and **1-Cl** (Cl analogue of **1**) were studied for comparison. The antiproliferative activity of complexes was also determined in monolayer cultures treated with the drugs for the same times (Tables 1 and 2, Fig. S2).

Our experiments show that **1** is highly effective in inhibiting tumour growth, being over $50\times$ and $15\times$ times more active than cisplatin and **1-Cl** (after 48 h treatment), respectively. As expected, this pattern is also observed for cell monolayers treated with these complexes. Interestingly, increases in the time of exposure of both 2D and 3D cultured cells to **1** (from 16 h to 48 h) led to comparable increases in antiproliferative activity: $8\times$ and $7\times$ times more active in cell monolayers and spheroids, respectively. This was not observed when cells were treated with cisplatin or **1-Cl**; longer exposure times led to dramatically higher improvements in the biological activity of cisplatin

and **1-Cl** in cell monolayers compared to 3D spheroids (Fig. S3). Overall, this suggests that **1** penetrates into spheroids in an efficient time-dependent way. To investigate this, microfocus x-ray fluorescence imaging experiments were carried out to map the distribution of osmium in the spheroids.

Synchrotron x-ray fluorescence (SXRF) was used to study the tumour spheroid penetration properties of osmium from complex **1** in A2780 spheroids treated with $0.7 \mu\text{M}$ **1** ($1/2 \times \text{IC}_{50\text{-sph}}$) for 0, 16, 24 and 48 h. Cells were fixed with glutaraldehyde, dehydrated with ethanol and embedded in resin for ultramicrotomy. Chemical fixation is not ideal for the preservation of biologically relevant elements in adherent mammalian cells [27], but it is required to produce thin sections for elemental analysis of spheroids and tissues. Elemental maps of 500 nm-thick sections of each sample were acquired on beamline I18 (DIAMOND Light Source, UK) [28]. The beam was focused to a $2 \times 2 \mu\text{m}^2$ size, and energy fixed at 12 keV to achieve excitation of the Os L_{III} -edge. The presence of Os in samples treated with **1** was confirmed by detection of the Os L_{III} X-ray fluorescence emission lines (Fig. S4).

Interestingly, the results suggest that **1** penetrates into the tumour core, and remains there for longer than expected. Although the background contribution could not be totally eliminated by peak fitting, maps of $300 \times 300 \mu\text{m}^2$ areas of interest (ROIs) collected from the different samples (step size $2 \times 2 \mu\text{m}^2$, dwell time 1 s; Fig. 1, Figs. S5–S8) showed that there is a direct relation between cell treatment time and tissue penetration of the complex (Figs. 1–2, Fig. S6). **1** occupies similar areas of the spheroids after 24 h and 48 h treatment. About 18% of the area studied contained Os (Fig. S9). However, Os penetrates more deeply into the tumour model (Fig. 2), and is accumulated more after $48 \text{ h} > 24 \text{ h} > 16 \text{ h}$, with levels of $6.4 \pm 1.6 > 4.8 \pm 0.7 > 0.11 \pm 0.02 \text{ pg Os/section}$ respectively (Fig. S10). In contrast, cell monolayers showed maximum uptake of **1** after 24 h incubation, followed by a rapid decrease in the amount of Os inside cells during the next 48 h [29]. Differences in the accumulation kinetics of **1** between cell monolayers and 3D tumour models may result from more effective efflux from cell monolayers, or slow diffusion of the drug into tissue-like samples.

The correlation between incubation time and amount of Os at the core of the spheroids, suggests that **1** is internalised by transcellular transport mechanisms. This means that the drug would be taken up by cells at the surface of the tumour and then moves towards more internal areas, being activated in the process. To investigate this, X-ray Absorption Spectroscopy (XAS) spectra were collected in areas with relatively high concentrations of Os within different parts of the spheroids. Well defined X-ray Absorption Near Edge Structure (XANES) and weak Extended X-Ray Absorption Fine Structure (EXAFS) for Os were observed (Fig. 3). However, S/N ratio was too low, most likely due to the low concentration of Os in the sample, and did not allow the meaningful fitting of the spectra. Attempts to use longer or multiple acquisitions to increase the S/N ratio led to a rapid decrease in the intensity of the XAS spectra, even when attenuators were used. This is likely to be due to beam damage of the sample, and hampered use of XAS to study the cellular speciation of **1**.

Treatment of spheroids with **1** also led to extensive changes in Zn and Ca distribution, from being discretely localised in untreated samples to being more widely distributed in treated spheroids (Fig. 1, Fig. S7–S8). This change in distribution was time-dependent. After 16 h exposure to the drug, some Zn and Ca are still discretely localised in certain areas of the spheroids, whereas after 24 or 48 h incubation, they are more evenly distributed. This is probably not the result of an increase in metal leaching from spheroids during sample preparation, as the total amount of Zn remained mostly unchanged across the different

Download English Version:

<https://daneshyari.com/en/article/7753681>

Download Persian Version:

<https://daneshyari.com/article/7753681>

[Daneshyari.com](https://daneshyari.com)